A 3D-printed, dynamic, patient-specific knee simulator

A 3D-Printed, Dynamic, Patient-Specific Knee Simulator

Abstract

Purpose

3D-printed devices proved their efficacy across different clinical applications, helping personalize medical treatments. In this paper, we present the procedure for the design and production of patient-specific dynamic simulators of the human knee. The scope of these simulators is to improve surgical outcomes, investigate the motion and load response of the human knee, and standardize in-vitro experiments for testing orthopedic devices through a personalized physical representation of the patient's joint.

Design/methodology/approach

We tested the approach on three volunteers. For each, a patient-specific mathematical joint model was defined from an MRI of the knee. The model guided the CAD design of the simulators, which was then realized through stereolithography printing. Manufacturing accuracy was tested by quantifying the differences between 3D-printed and CAD geometry. To assess the simulator functionality, its motion was measured through a stereophotogrammetric system and compared with the natural tibio-femoral motion of the volunteers, measured as a sequence of static MRI.

Findings

The 3D-printing accuracy was very high, with average differences between ideal and printed parts below ± 0.1 mm. However, the assembly of different 3D-printed parts resulted in a higher average error of 0.97 mm and peak values of 2.33 mm. Despite that, the rotational and translational accuracy of the simulator was about 5° and 4 mm, respectively.

Originality/value

Although improvements in the production process are needed, the proposed simulators successfully replicated the individual articular behavior. The proposed approach is general and thus extendible to other articulations.

Keywords

Knee, Dynamic Simulator, 3D-printing, Patient-Specific

Paper type: Research Paper

Funding information: This research study was funded by the NSF IRES Track I Award # 1827075

Declarations: Ethics approval and consent to participate: Experimental MRI measures were performed on volunteers

Consent for publication: Authors give necessary conesent for publication in the Journal

Conflict of interest: The authors declare no competing interests.

1. Introduction

In the last decade, 3D-printing spread across numerous surgical disciplines, helping analyse complex cases, practice procedures, and teach resident students (Banga *et al.*, 2022; Brumpt *et al.*, 2023; Chae *et al.*, 2015; Diment *et al.*, 2017; Fleming *et al.*, 2020; Tack *et al.*, 2016). In preoperative planning, 3D-printed biomodels have been successfully used in the field of maxillofacial and orthopaedic surgery, allowing for accurate reconstruction of bony defects and prefabrication of bony fixation plates. 3D-printing has been used to fabricate patient-specific devices for surgical guidance, also enabling the rapid and convenient production of customized implants. All medical fields that assessed 3D-printed devices concluded that they were clinically effective, decreasing surgical operation times and increasing surgical accuracy (Diment *et al.*, 2017). 3D-printed models also achieved good success as educational tools. Several studies have demonstrated the advantages of 3D-printed models both instead of and in addition to traditional educational methods (Langridge *et al.*, 2018; Smith *et al.*, 2018; Ye *et al.*, 2020). Several companies have established business on 3D-printed biomodels.

Despite many successful clinical applications, most the 3D-printed models are static anatomical replicas, unable to represent the dynamic spatial relationships between different anatomical structures (Cai *et al.*, 2019; Clifton *et al.*, 2021). On the other side, such dynamic models would resent a valuable preclinical tool, particularly in orthopaedics, where the combination of medical images and 3D-printing would allow for the realization of patient-specific replicas of the joint to be treated. These models would allow, for example, to evaluate the impact of different implants and their alignments on the final joint kinematics for a specific patient, before entering in the operating theatre. In this context, the knee joint provides an interesting first application. Indeed, literature report a 20% of dissatisfaction among the total knee arthroplasty (TKA) patients (Bourne *et al.*, 2010; Gandhi *et al.*, 2007; Gunaratne *et al.*, 2017a; Noble *et al.*, 2006). Considering that primary TKA is projected to grow up to 1 million procedures per year and replacement TKA is projected to grow up to 100-200 thousand procedures per year by 2030 in the US alone (Schwartz *et al.*, 2020; Sloan *et al.*, 2018), there is a substantial interest to explore new patient-specific tools for the identification of the causes of patient dissatisfaction and improve TKA surgical outcome (Choi and Ra, 2016; Gunaratne *et al.*, 2017b; Kim *et al.*, 2009; Scott *et al.*, 2010).

Despite the clear need for a personalized functional simulator of the knee, to our knowledge only two examples are available in the literature. The first (Mercader *et al.*, 2021) is however a planar simplification, modelling the patient motion only in the sagittal planes by means of the well-known 4-bar linkage, missing the internal/external and ab/adduction rotation, and the medial/lateral translation of the knee. Also, the simulated kinematics is rigidly dictated by the mechanism and thus it does not respond to surgical modifications. The second simulator (Cai *et al.*, 2019) provides a finer 3D model of the knee, including simplified articular surfaces and the four principal ligaments in the knee, these latter represented with cables. This simulator has the merit to replicate the spatial tibiofemoral motion, including the internal/external rotation. It is however generic and not easily adaptable to the anatomy of the single patient.

The lack of patient-specific dynamic simulator can be explained considering that their design requires a mathematical model that identify the constraints that govern the articular behaviour and sensitive to the anatomical variability among individuals. Joint motion and response to load is mainly dictated by articular surfaces and soft tissues. While a three-dimensional representation of the formed can be obtained easily from standard medical images, the correct identification of ligament insertions and resting lengths is a more complex task. Indeed, ligaments characteristics and are normally indirectly reconstructed from physiological assumptions or complex experimental measures (Erdemir *et al.*, 2019). Recently, new knee models have been introduced that predict

individual joint motion from the shape of the articular surfaces, also allowing the identification of ligament characteristics in terms of insertions and resting length (Conconi *et al.*, 2019, 2022a; Conconi, Sancisi, *et al.*, 2021a, 2021b; Martelli *et al.*, 2020; Nardini *et al.*, 2020a). Starting from standard clinical images, it is thus possible to reconstruct a 3D representation of the patient anatomy, from which a personalized model can be defined, opening the way to the design of new, personalized knee dynamic simulators. These latter could help to improve surgical outcomes, by allowing the surgeon to compare various knee implant designs or different alignments of the same implant prior to surgery on the specific patient, providing a better feeling for the surgeon with respect to digital models. Such simulators could also represent a valid teaching tool for surgeons, adding to the proven benefits of 3D-printed anatomical models (Ye *et al.*, 2020) the possibility to investigate the motion and response to load of the human knee, for instance representing a replica of rare pathologies or clinical cases. Finally, the simulators can be used as an additional platform to standardize in-vitro experiments for testing orthopaedic devices, allowing a considerable reduction of the costs and time of preclinical tests (Diment *et al.*, 2017).

The aim of this paper is to propose and validate a procedure for the realization of patient-specific dynamic knee simulators by means of additive manufacturing. To validate the approach, we built three simulators from different volunteers: for each, a MRI of the knee was acquired to provide the reference anatomy for the patient-specific knee model. The natural tibio-femoral motion of each volunteer was also measured to provide a reference motion. We tested the manufacturing accuracy by quantifying the differences between 3D-printed and CAD geometry of bones and articular surfaces. To evaluate the functionality of the simulators, we measured the tibio-femoral kinematics and compared it with the knee natural motion of the volunteer. Finally, to provide a possible clinical application, we used the simulator to test a personalized knee implant design.

2. Materials and Methods

2.1. Definition of individual knee model

The natural motion of the knee implies the isometry of all the ligaments that guide its motion (Conconi *et al.*, 2019). Once that a reference motion and a representation of the articular anatomy of an individual has been provided, it is possible to identify the single most isometric fiber in each ligament. The reference motion can be predicted using a personalized joint model capable to reconstruct the knee kinematics from the individual anatomy (Conconi *et al.*, 2022b; Conconi, Sancisi, *et al.*, 2021c). In this study a direct measure of articular motion was recorded for each subject to provide a stronger validation of the design procedure. With this anatomic and kinematic information, it is possible to synthesize parallel mechanisms whose motion will be equivalent to the patient's knee (Nardini *et al.*, 2020a). These mechanisms are thus useful tools to define personalised medical mechanical devices and have been used to define patient-specific implants (Parenti-Castelli *et al.*, 2010). They are used here to define the geometry of the simulators.

We investigated the knee from three volunteers (age: 29 ± 7.9 years; height: 174. 3 ± 7.6 cm; weight: 71.7 ± 7.6 kg). For each one, an initial MRI of the knee (3D hybrid contrast enhancement, FOV 512x512, pixel spacing 0.5/0.5, slice thickness 0.5 mm, TR = 10 ms, TE = 5 ms, flip angle 60°, hereinafter 3D HYCE) was taken within a 0.25 T G-Scan, Esaote SpA.

Articular cartilages, ligament origins and insertions, and bones were segmented for the femur, tibia, and fibula through the open software MITK, to obtain 3D STL representations of three volunteers' anatomy. Anatomical reference systems for the femur and tibia were defined based on the convention proposed by Tashman et al. (Tashman and Anderst, 2003), for which x, y, and z are axes respectively pointing anteriorly, proximally, and to the right. Tibio-femoral pose was expressed according to the Grood

and Suntay convention (Grood and Suntay, 1983), obtaining the abduction/adduction (AA), internal/external (IE), and flexion/extension (FE) joint rotations.

With the same MRI scanner, a series of 5 weight-bearing images were also acquired, varying the knee flexion angle approximately between 0° and 90° with an MRI compatible rig (Conconi *et al.*, 2023). The femur and tibia bones were segmented from each scan and the STL models from the static MRI were aligned to them through bone-to-bone registration, allowing for the reconstruction of the individual knee kinematics by five poses (Figure 1).

Once that patient motion and anatomy have been provided, the most isometric fibers are identified as the line connecting two points, one in the origin and the other in the insertion of each considered ligament, whose relative length variation is minimal along the reference motion:

$$\Delta L = \frac{L_{max} - L_{min}}{L_{max}}$$

where L_{max} and L_{min} are the maximum and the minimum fiber length measured during the motion, respectively. In this case, 6 main ligaments were considered: the anterior and posterior cruciate ligaments (ACL and PCL, respectively), the lateral and medial collateral ligaments, this latter divided into deep and superficial layer (LCL, MCLd, and MCLs, respectively), and the antero-lateral ligament (ALL). Origin and insertion of isometric fibers dictated the via points for the cables emulating the ligaments in the 3D-printed simulator.

Based on the procedure in (Nardini et al., 2020), an equivalent parallel mechanism was synthesized for each knee, and then used to design a custom knee implant for each volunteer according to ("Parenti-Castelli, V., Catani, F., Sancisi, N., & Leardini, A. (2010). Improved orthopaedic device. PCT Patent WO2010/128485.", n.d.).

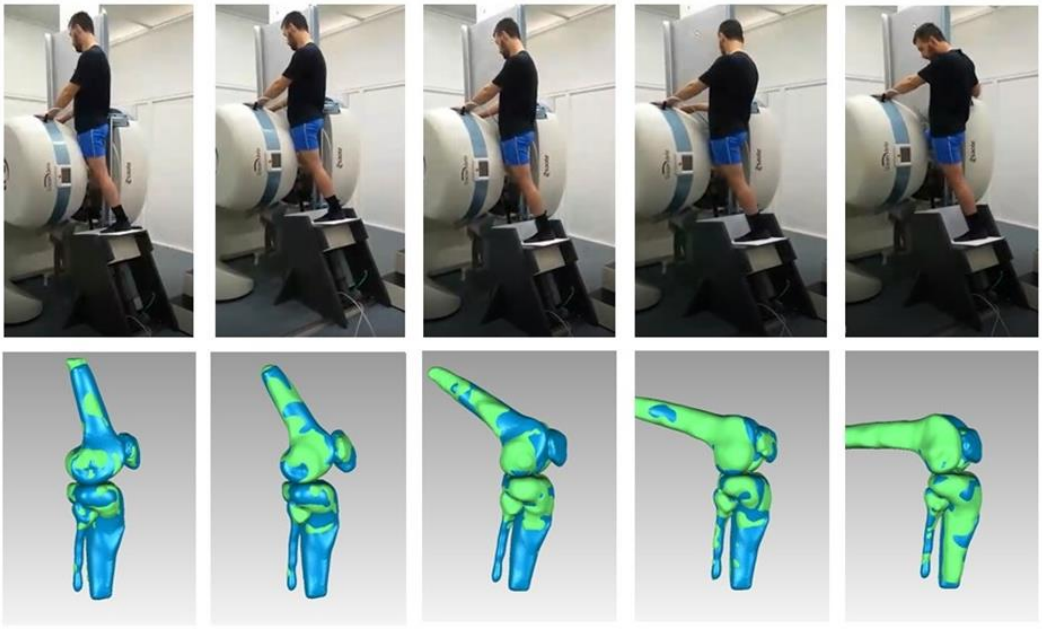

Figure 1. Reconstruction of knee kinematics from 5 weight-bearing scans at different knee flexion angles. Patient position for each scan (top row) and corresponding segmentation of knee bones (bottom row). The bones from initial MRI are represented in green, registered on the corresponding bones as segmented from each weight-bearing MRI, in blue.

2.2. Simulator Design

The STL models derived from static MRI were utilized in the design of the simulator and knee implants. Rhinoceros 3D (Rhino) (Robert McNeel & Associates, Seattle, WA) was

used to merge the STL models and design simulator features, which include interchangeable articular surfaces, a ligament tensioning system, and reference bases for aligning the femur and tibia components in the anatomical reference configuration during the assembly of the simulator.

The interface between the interchangeable articular surface and the bone base was defined using surgical cut planes, to obtain a more realistic implant design and surgery simulation. The articular surfaces were made interchangeable by means of press fit pins. The anatomical surfaces were designed by splitting the articular surfaces of the femur and tibia STL files at the surgical cut planes. The knee implant articular surfaces were designed starting from the geometry of the femur. According to the considered knee design, the femoral knee implant was defined by modifying articular surfaces with a spherical surface on the medial condyle and a conical surface on the lateral condyle (Figure 2). The tibia knee implant was defined by generating the negative of a sweep of the femur knee implant at all poses defined from the patient's full range of motion (Figure 2). The thickness of the resulting implants ranges approximately from 1 to 15 mm (Figure 3). The modularity of the articular surfaces augments the clinical usability and impact of the simulator.

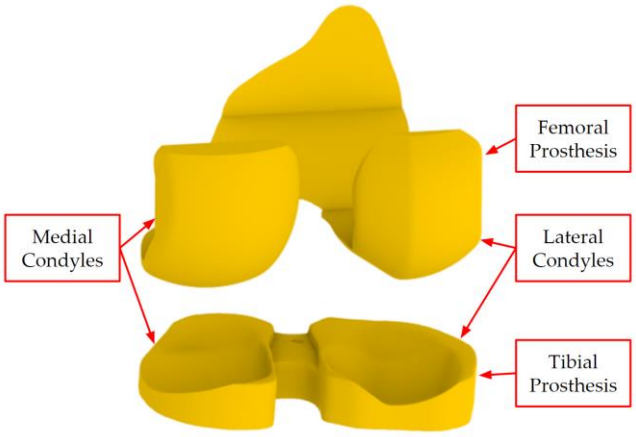

Figure 2. Femoral and tibial knee implant designs

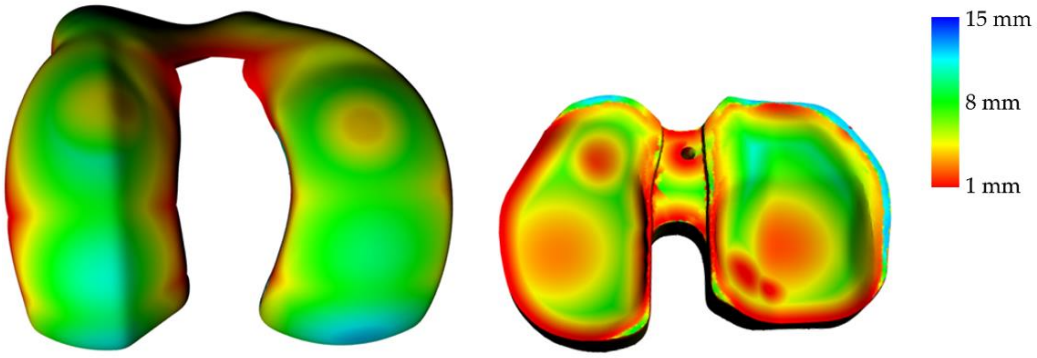

Figure 3. Femoral and tibial knee implant thickness analysis

The ligament tensioning systems are anchored to the reference bases, simplifying the assembly while reducing the risk of interference during motion. Thru-holes link ligament attachment points to the tensioning system, which uses tuning machine heads to provide a compact way of tune and hold ligament. This system also makes it possible to cope with construction inaccuracy and cable elasticity and relaxation (Figure 4) Part dimensions are reported in Table I. The system attaches to the bone bases with screws and screw-to-expand inserts, which are simple to use and compatible with 3D-printed parts (Figure 5).

The reference bases were added at the proximal and distal end of femur and tibia bone models, respectively. Two planes on these bases are defined so that they are aligned (parallel and coincident) when the knee is at the extension reference pose taken in the MRI (Figure 4). This provides an anatomical position of the femur and tibia, and a correct tensioning of the ligaments during assembly.

Hereinafter, the parts including the bones and the bases will be called simply "bones", while the interchangeable parts, representing either the articular surfaces of the volunteer personalized knee implants, will be called "articulating surfaces".

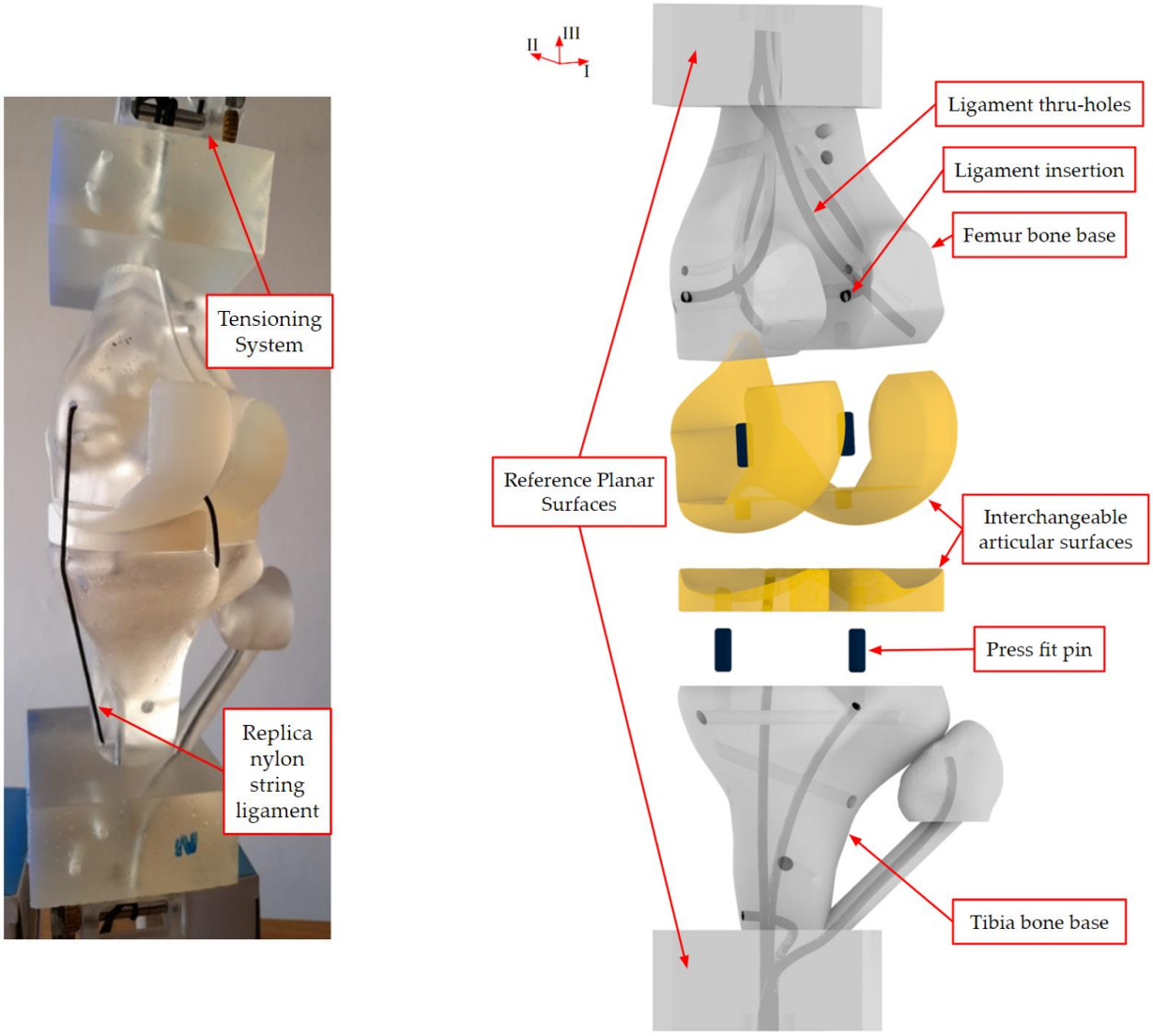

(**a**) (**b**)

Figure 4. (**a**) Simulator assembled with tensioned replica ligaments; (**b**) exploded view of simulator assembly

Table I. Average part dimensions (unit: mm).

Dimension (as shown in Figure 4b)	Femur bone base	Femoral Prosthesis	Tibia bone base	Tibial Prosthesis	Press fit pin
I	110.5	84.4	110.6	81.4	4.9
II	106.4	76.9	106.9	55.3	4.9
III	106.0	56.0	107.7	17.1	11.0

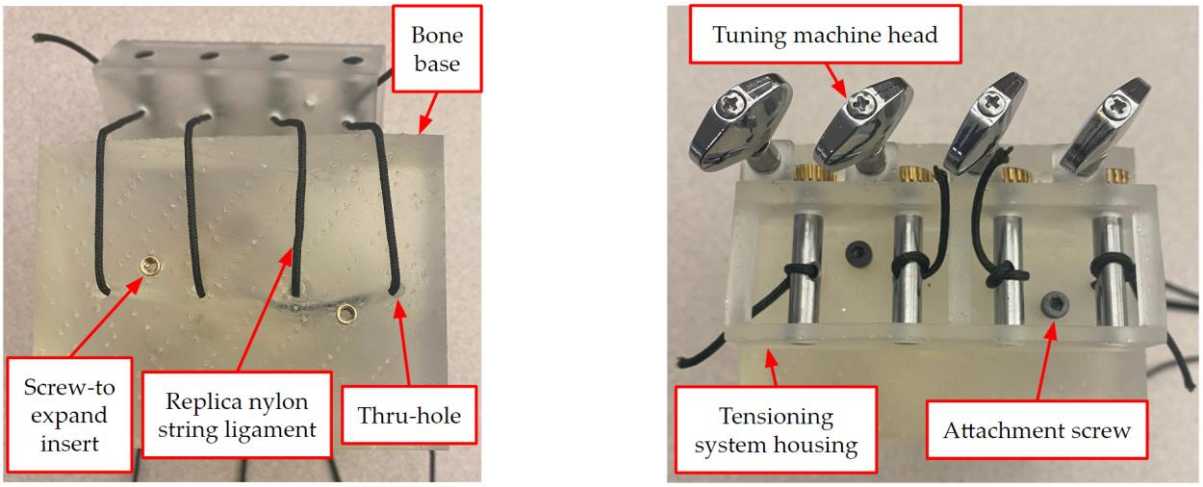

(**a**) (**b**)

Figure 5. (**a**) Tensioning system detached from base; (**b**) tensioning system attached to base

2.3. Printing Methodology

2.3.1 Material Selection

In the absence of relevant loads, 3D-printing materials can be chosen to reduce friction, thus enabling a better approximation of joint behavior. Stereolithography (SLA) printing was selected due to its dimensional accuracy and print resolution (Lakkala *et al.*, 2023; Melchels *et al.*, 2010; Ngo *et al.*, 2018; Raman and Bashir, 2015). In a preliminary investigation, two resins, Formlabs' (Somerville, MA) Durable and Clear Resins, were studied to understand their functionality within the confines of the proposed simulator. Friction testing with a weighted sled and track, showed that Durable Resin and Clear Resin had significantly different coefficients of static friction ($p = 0.007$) of 0.18 and 0.28, respectively.

To validate the friction testing in a functional scenario, knee implant components were 3D-printed in both resins and articulated by hand. The Clear Resin knee implant were found to have difficulty during actuation with observed high friction and noticeable wear (Figure 6) when compared with Durable Resin knee implants. This analysis confirmed previous friction testing results and suggested the use of Durable Resin was more adequate for the simulator. Articulating components were printed with Durable Resin to promote smoother actuation while other parts of the knee model were 3D-printed with Clear Resin as they did not require low friction properties and reduced the cost of the simulator.

(**a**) (**b**)

Figure 6. (**a**) Clear resin knee implants showed noticeable wear after testing on both the lateral and medial condyles as well as the tibial plateau; (**b**) durable resin knee implants showed no visible wear after testing.

2.3.3. 3D-Printing Parameters

A Form 3 Printer (Formlabs, Somerville, MA) was utilized to conduct these prints. PreForm software (Formlabs, Somerville, MA) was used to visualize and adjust the printing parameters and ensure optimal results. All parts were printed with a 0.050 mm layer thickness with auto-generated full raft supports at a density of 1.00. Support touchpoint size was 0.70 mm for Durable Resin parts and 0.50 mm for Clear Resin parts. Internal supports were not used when printing bones to avoid obstructing ligament thru-holes.

Printing orientation was determined to avoid or minimize the presence of supports on articular and reference surfaces (Figure 7). Additional supports were manually placed along the anterior and posterior cut planes of knee implant components to increase support density, in order to strengthen the part and help reduce deformation during curing and postprocessing as needed (Figure 7). The tibial knee implant was oriented at an angle to avoid "cupping blowout" during printing, which can lead to print failure ("Cupping blowout", 2020) (Figure 7). The bones were oriented at an angle so that the entirety of the ligament thru-holes' axes and of planar surfaces were non-parallel to the print bed. This increases print fidelity and decreases the likelihood of hole collapse (Jang *et al.*, 2023; McCarty *et al.*, 2020; Park *et al.*, 2019; Unkovskiy *et al.*, 2018).

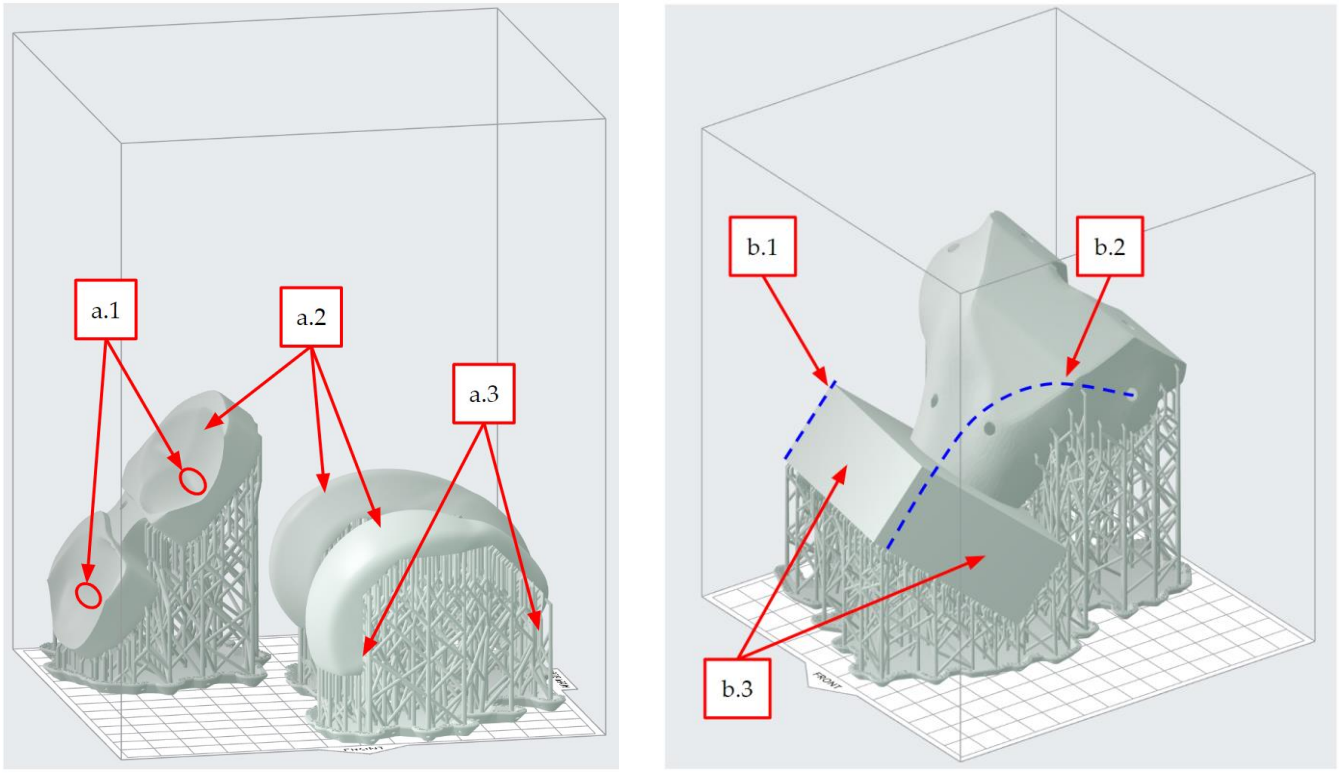

(**a**) (**b**)

Figure 7. (**a**) (a.1) Knee implants angled to avoid cupping during printing at these locations (a.2) supports are not placed on the lateral condyle, medial condyle, and tibial plateau (a.3) extra supports placed along anterior and posterior cut planes; (**b**) (b.1) planar surfaces are non-parallel to the print bed (b.2) ligament thru-hole axes were oriented non-parallel to the print bed (b.3) supports are not placed on planar alignment surfaces

2.3.4 Print Curing

Curing parameters including the presence of UV light, heat, and time were assessed to achieve successful prints. UV curing is needed for resin-based 3D-printing techniques such as SLA, but part deformation can occur after this process (Fuh *et al.*, 1997; Katheng *et al.*, 2021; Wang *et al.*, 1996; Zhao *et al.*, 2020). Multiple copies of knee implants were printed and tested with varying curing parameters. It was observed that fast curing (15-60 minutes) using heat (0-60°C) and UV light caused the part to warp consistently over ten trials. As a result, further investigation was conducted to assess the viability of slow

curing the component, deviating from the manufacturer's recommended curing conditions, while applying geometric constraints. This testing found optimal curing for knee implants was achieved by initially allowing them to sit at room temperature for a week while securely attached to the bone bases to maintain shape during slow curing. The knee implants were then placed in UV light with no additional heat for 20 minutes to further cure and harden the outer contact surfaces of the knee implants to reduce friction. Bones and other parts were cured according to recommendations of Formlabs (Somerville, MA).

2.4. Experimental Validation

A stereophotogrammetric system (Vicon; 6 Bonita, 2 Vero cameras) was used to measure simulators' motion and printing accuracy. The system was set up as described in (Conconi, Pompili, *et al.*, 2021). Briefly, calibration was performed using at least 3000 frames per camera, performing acquisitions at 100 Hz, using Polaris retro-reflective passive markers, 11.5 mm in diameter. Cameras were distributed evenly on a circular arch, concentric with the calibrated volume centre, symmetrically varying their heights (Figure 8), to maximize the system accuracy (Windolf *et al.*, 2008), that with this setup has been quantified as 0.11±0.07 mm for a single marker position (Conconi, Pompili, *et al.*, 2021). Two rigid trackers, each featuring three markers, were screwed to the femur and tibia (Figure 8). The tibia was then clamped to the laboratory table and the femur was manually flexed by means of a stick, to minimize the force applied to the system. Flexion was repeated 5 times using anatomical surface replicas as articulating surfaces. Then, the simulator was disassembled, and the 3D-printed custom knee implant surfaces were used. The measure was then repeated. Prior to any motion, the surface of bones and articulating surfaces were digitized by means of a pointer (Figure 8), whose accuracy can be quantified as below 0.3 mm, given the system accuracy and the pointer geometry. The tibio-femoral relative kinematics was reconstructed from the trackers' motion and expressed using anatomical reference systems, whose pose relative to the tracker was obtained by registering the STL bone models on the corresponding point clouds using a standard iterative closest point (ICP) algorithm.

To quantify the printing accuracy, the clouds of points were registered independently on the corresponding STL model, i.e., bones and articulating surfaces were analyzed separately. To quantify the assembly accuracy of articulating surfaces, for each bone, the clouds of points of the articulating surface and bone were joined as a single cloud and registered on the assembled STL model, using only the bone cloud and STL to perform registration. Both printing and assembly accuracy were quantified as the mean error between digitized points and STL corresponding models. Positive and negative errors represent points outside or inside the theoretical STL surface.

To quantify the simulator accuracy in replicating the knee kinematics, the differences between the simulator and experimental MRI poses were evaluated at the five flexion angles corresponding to the five weight-bearing MRI scans. At each pose orientation and position error were defined as

$$\Delta\theta = \sqrt{(AA_{sim} - AA_{MRI})^2 + (IE_{sim} - IE_{MRI})^2}, \quad (1)$$

$$\Delta P = \sqrt{(X_{sim} - X_{MRI})^2 + (Y_{sim} - Y_{MRI})^2 + (Z_{sim} - Z_{MRI})^2}, \quad (2)$$

where the subscripts denote simulator and MRI experimental measurements.

The simulator rotational and translational accuracy were finally defined as the average rotational and translational error over the five poses and the five repetitions.

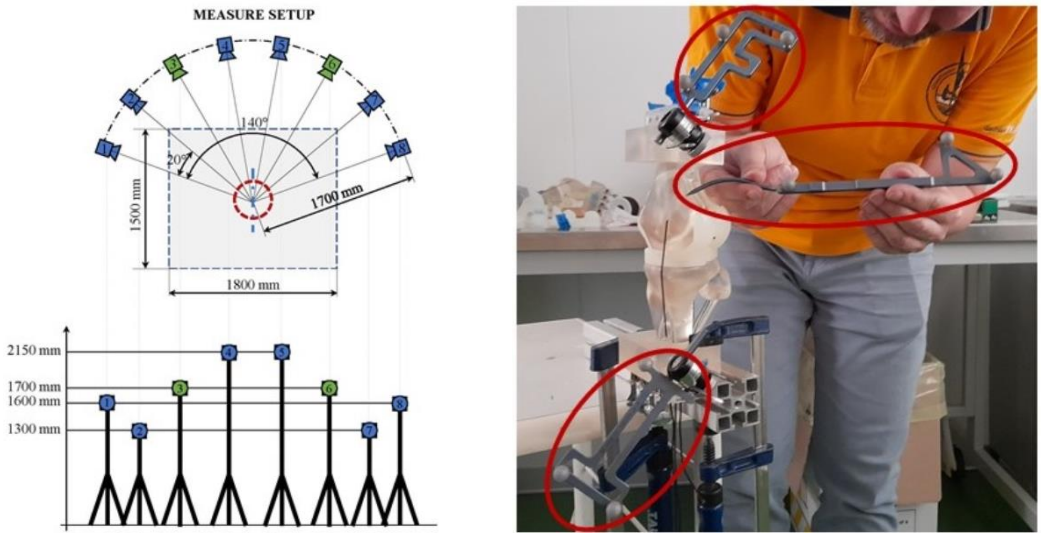

(**a**) (**b**)

Figure 8. (**a**) Schematic representation of the camera distribution for the stereophotogrammetric system; (**b**) example of the experimental setup, in which the trackers and the pointer are enlightened.

3. Results

The average deviation between theoretical surfaces and digitized point clouds are summarized in Table II, both for the printing and assembly accuracy, as defined above. Figures 8 and 9 show the same comparison graphically.

In general, printing accuracy of single parts is very high, the average error being below 0.1 mm both for bones and articulating components. On the contrary, assembly accuracy revealed an average error of 0.97±0.73 mm, well above the measurement accuracy, with a peak of 2.33±1.08 mm for the femur with personalized implant of Subject 1.

Table II. Printing and assembly accuracy for the three subjects (unit: mm).

		Bone printing accuracy	Printing accuracy: Subject articular surface	Printing accuracy: Personalized implant	Assembly accuracy: Subject articular surface	Assembly accuracy: Personalized implant
Subject 1	**Femur**	-0.01±0.35	-0.01±0.32	-0.01±0.15	0.99±0.73	2.33±1.08
	Tibia	-0.02±0.27	-0.02±0.33	-0.01±0.24	2.00±0.62	1.51±1.02
Subject 2	**Femur**	-0.11±0.44	-0.40±1.37	0.01±0.22	0.87±1.33	1.35±0.70
	Tibia	0.01±0.46	-0.06±0.27	-0.03±0.30	0.89±0.61	0.69±0.70
Subject 3	**Femur**	-0.02±0.39	0.01±0.17	-0.02±0.17	0.63±0.90	0.69±0.47
	Tibia	-0.14±0.73	-0.01±0.17	0.00±0.06	-0.17±0.29	-0.08±0.27

	Bone printing accuracy	Surface printing accuracy	Assembly accuracy
Average	-0.05±0.44	-0.04±0.31	0.97±0.73

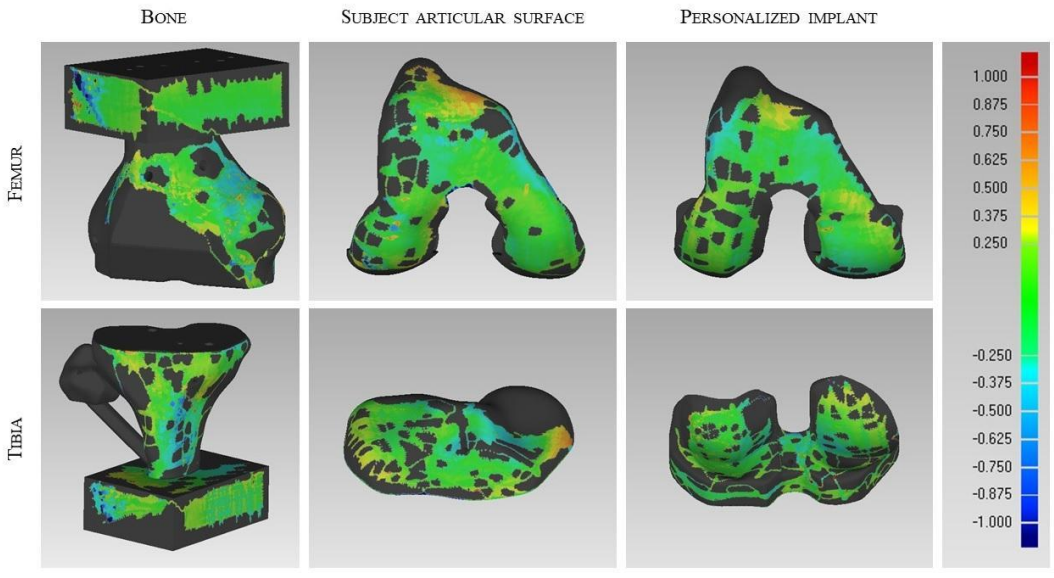

Figure 9. Distance maps between clouds of digitized points and corresponding STL, after ICP registration.

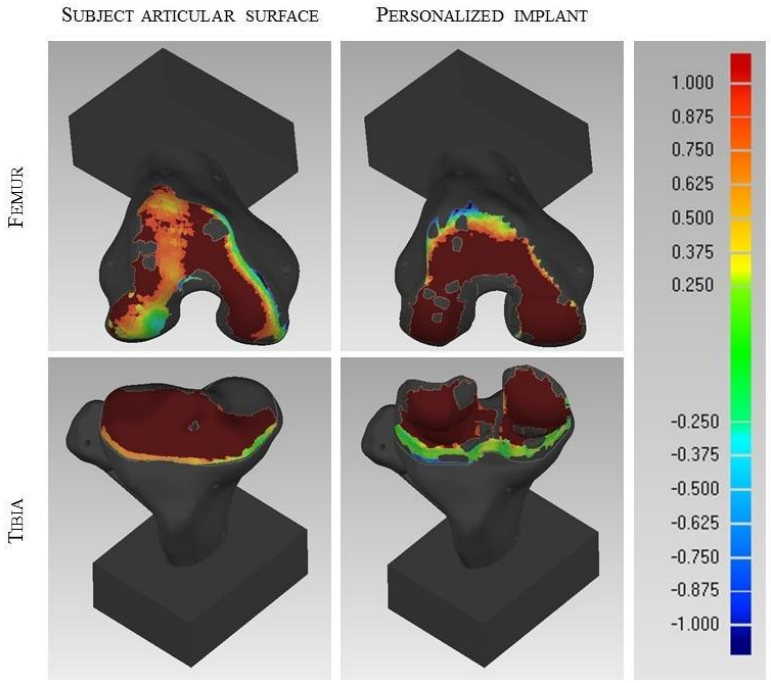

Figure 10. Distance maps between the point clouds of articulating surfaces as registered on the assembled STL model, using only the bone cloud and STL to perform registration.

Figure 11 shows the comparison between the volunteer natural motion, as measured through MRI, and the motion of the simulator, both with the subject articular surfaces and the personalized implants. The rotational and translational accuracy of the simulator is reported in Table II.

In general, the simulator replicates well the natural motion of the different knees: although some differences are observable, these are mainly constant offsets with the curves showing similar trends. The overall average rotational and translational accuracy were about 5° and 5 mm, respectively.

Table III. Rotational and translational kinematic accuracy for the tested knee simulators (unit: mm).

	Errors	Subject articulating surface	Personalized implant
Subject 1	Δθ	4.94±3.92	5.08±0.91
	ΔP	2.94±0.62	3.23±4.22
Subject 2	Δθ	5.68±1.83	5.67±1.83
	ΔP	3.57±0.75	3.63±1.15
Subject 3	Δθ	4.59±1.85	3.32±1.68
	ΔP	5.20±0.39	5.05±1.48
Average	Δθ	5.07±2.56	4.69±1.75
	ΔP	3.90±1.14	3.97±2.60

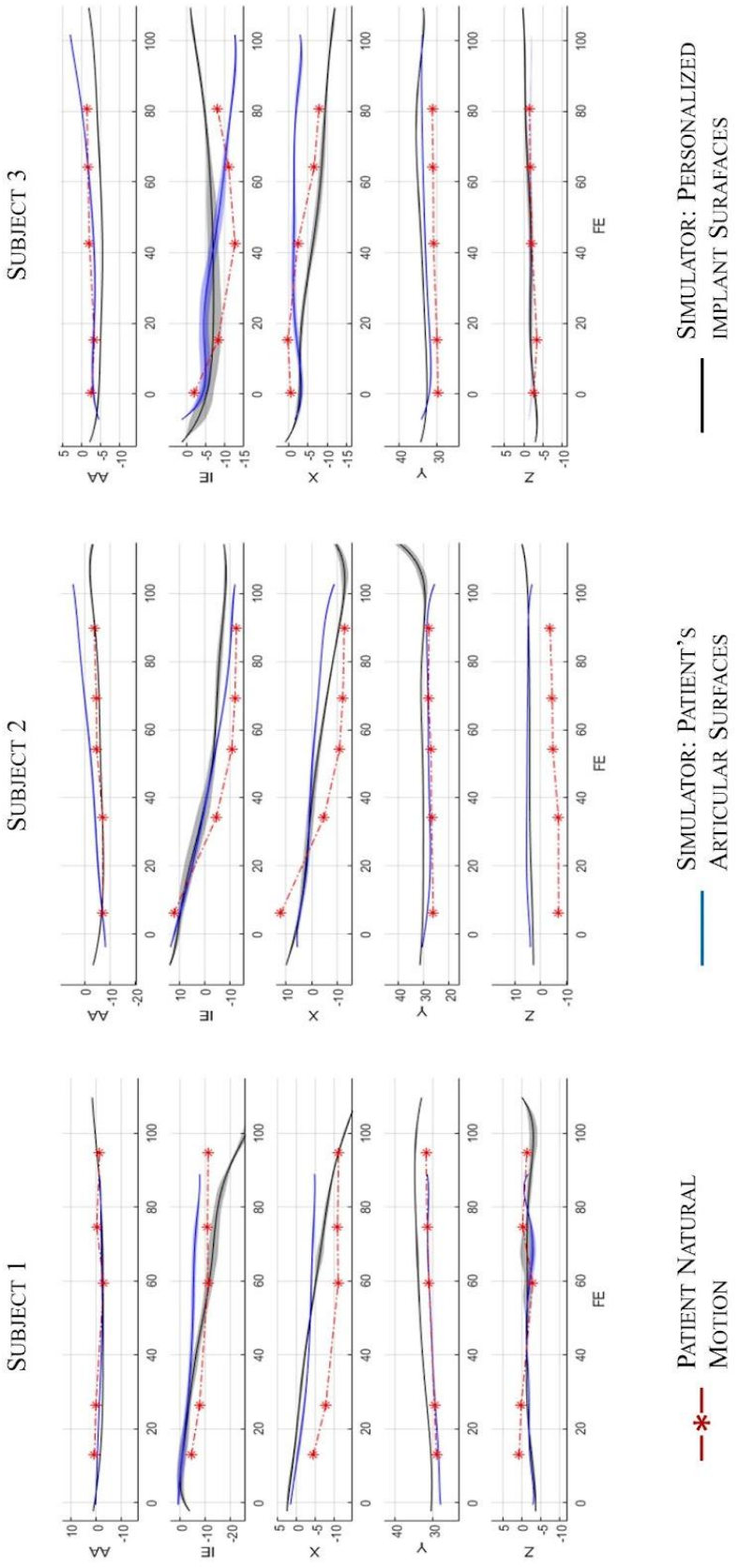

Figure 11. Comparison between patient natural motion as measured through orthostatic MRI (red dotted line), simulator with patient's articular surface (blue line), and simulator with personalized implant (black line) (unit: mm).

4. Discussions

In this paper, we presented the procedure for the design and production by 3D-printing of patient-specific dynamic simulators of the human knee. The design procedure starts by segmenting medical images to extract anatomical surfaces, the latter used to predict patient-specific joint kinematics by means of mathematical models presented in (Conconi *et al.*, 2022b; Conconi, Sancisi, *et al.*, 2021c). From here, it is possible to identify the most isometric fibres of each considered ligament, which will provide the anchor point for each cable representing a ligament in the simulator. Finally, the simulator components are designed by combining the STL model of bones with cartilage and ligament anchor points, adding additional features such as a tensioning system and reference surfaces for the correct assembly of the simulator. For the definition of the patient-specific implant, a parallel mechanism kinetostatically equivalent to the patient articulation was defined (Nardini *et al.*, 2020a) and then used to synthetise personalized implant surfaces (Parenti-Castelli *et al.*, 2010). STL models of one simulator are made available with the present paper to test the approach. However, the procedure for the simulator design is totally general and can be used in combination with different prostheses or surfaces.

In this work, we experimentally tested the simulators to verify both the manufacturing accuracy and their capability to replicate individual joint motion. The 3D-printing accuracy was very high, with average differences between ideal and printed parts below ± 0.1 mm for all components. The technology, the material and the production parameters are therefore suitable for this application.

On the contrary, the assembly of different 3D-printed parts resulted in significant errors, with an average deviation from theoretical surfaces of 0.97 mm and peak values of 2.33 mm for one femoral component of the personalized implant. This may be the effect of residual imperfections remaining after the removal of the supporting structures, which were insisting on the coupling surfaces of articular parts (Figure 7.a). To test this hypothesis and as a possible mitigation of this issue, future investigations will be carried out by realizing bone and corresponding articulating surface as a single object.

The kinematic accuracy of the simulators is in general good. The simulator replicates the characteristic motion of the knee, with internal rotation and roll back of the femur during flexion; also, resulting kinematics changes from subject to subject, showing the capability of the simulator to capture anatomical variability. The same behavior is shown by the knee implants, which allow a good restoration of the original kinematics. On the one hand this shows the possibilities of these simulators in analyzing the impact of a knee implant on the patients; on the other hand, it shows the potential of personalized implant design.

Some differences between natural and simulator motion are observable, though resulting mainly in constant offsets. Differences of this nature are reasonably ascribable to the assembly inaccuracies which, combining the tibia and femur assembly errors, reach on average 2 mm, with possible higher peaks. These kinds of errors alter the ligament reference length, with a considerable impact on the whole kinematics. In this perspective, the capability of the simulator to still correctly reproduce the characteristic pattern of the knee motion is highly encouraging though it requires improvements in the production process. Again, tests on single printed bone and articular surfaces will help verify this hypothesis.

This work has limitations. The number of volunteers is limited however, considering the context of a feasibility study, it is sufficient to support the soundness of the proposed approach. A complete characterization of the simulators response to loads is also needed and will be performed in the future, resorting the specific rig developed for the scope (Forlani *et al.*, 2016). In this sense, material properties of both printing material and ligament replica need to be further tailored to better match those of biological tissue, for instance resorting to material such as the Bone Matrix recently proposed by Stratasys (Wright *et al.*, 2023) and to electrospun, nanofibrous artificial replica of the ligaments, producing nanofibers similar to the natural collagen fibrils (Sensini and Cristofolini, 2018). However, even if the simulator stiffness has not been yet investigated and compared with

the physiological one, the capability to correctly replicate the individual patient kinematic provide a first fundamental validation with important clinical implications. In fact, to replicate the patient cinematics, the constraints exerted by the contacts and the ligaments in the simulator must be equivalent to those of the patient articulation. Therefore, the kinematic response of the presented simulator can be considered as indicative of the one of the real knee, will be able to capture how a given implant its alignment will interact with the remaining articular structures, thus providing valuable information to the surgeon out of the operating theater, for instance allowing to modify the alignment of an implant to optimize the balancing of the operated joint.

5. Conclusions

The proposed simulators were shown to be feasible devices for the replication of the patient's articular behavior and the prediction of the effect of medical devices, with time and cost compatible with clinical procedures.

These simulators may help surgical planning, allowing the surgeon to train for an operation and/or to compare different surgical techniques and devices.

Also, simulators may be used for teaching clinicians, in addition to more complex and expensive cadaver labs.

The proposed approach is general and thus extendible to other articulations in the future.

References

Banga, H.K., Kumar, R., Kalra, P. and Belokar, R.M. (2022), *Additive Manufacturing with Medical Applications*, CRC Press.

Bourne, R.B., Chesworth, B.M., Davis, A.M., Mahomed, N.N. and Charron, K.D.J. (2010), "Patient satisfaction after total knee arthroplasty: who is satisfied and who is not?", *Clinical Orthopaedics and Related Research®*, Springer, Vol. 468, pp. 57–63.

Brumpt, E., Bertin, E., Tatu, L. and Louvrier, A. (2023), "3D printing as a pedagogical tool for teaching normal human anatomy: a systematic review", *BMC Medical Education*, Springer, Vol. 23 No. 1, p. 783.

Cai, B., Rajendran, K., Bay, B.H., Lee, J. and Yen, C. (2019), "The Effects of a Functional Three-dimensional (3D) Printed Knee Joint Simulator in Improving Anatomical Spatial Knowledge", *Anatomical Sciences Education*, Vol. 12 No. 6, pp. 610–618, doi: 10.1002/ase.1847.

Chae, M.P., Rozen, W.M., McMenamin, P.G., Findlay, M.W., Spychal, R.T. and Hunter-Smith, D.J. (2015), "Emerging Applications of Bedside 3D Printing in Plastic Surgery", *Frontiers in Surgery*, Vol. 2, doi: 10.3389/fsurg.2015.00025.

Choi, Y.-J. and Ra, H.J. (2016), "Patient satisfaction after total knee arthroplasty", *Knee Surgery & Related Research*, Korean Knee Society, Vol. 28 No. 1, p. 1.

Clifton, W., Damon, A., Soares, C., Nottmeier, E. and Pichelmann, M. (2021), "Investigation of a three-dimensional printed dynamic cervical spine model for anatomy and physiology education", *Clinical Anatomy*, Wiley Online Library, Vol. 34 No. 1, pp. 30–39.

Conconi, M., De Carli, F., Berni, M., Sancisi, N., Parenti-Castelli, V. and Monetti, G. (2023), "In-Vivo Quantification of Knee Deep-Flexion in Physiological Loading Condition trough Dynamic MRI", *Applied Sciences*, Vol. 13 No. 1, p. 629, doi: 10.3390/app13010629.

Conconi, M., Pompili, A., Sancisi, N. and Parenti-Castelli, V. (2021), "Quantification of the errors associated with marker occlusion in stereophotogrammetric systems and implications on gait analysis", *Journal of Biomechanics*, Vol. 114, p. 110162, doi: https://doi.org/10.1016/j.jbiomech.2020.110162.

Conconi, M., Sancisi, N. and Parenti-Castelli, V. (2019), "The Geometrical Arrangement of Knee Constraints That Makes Natural Motion Possible: Theoretical and Experimental Analysis", *Journal of Biomechanical Engineering*, Vol. 141 No. 5, doi: 10.1115/1.4043028.

Conconi, M., Sancisi, N. and Parenti-Castelli, V. (2021a), "Prediction of Individual Knee Kinematics From an MRI Representation of the Articular Surfaces", *IEEE Transactions on Biomedical Engineering*, Vol. 68 No. 3, pp. 1084–1092, doi: 10.1109/TBME.2020.3018113.

Conconi, M., Sancisi, N. and Parenti-Castelli, V. (2021b), "The Geometrical Arrangement of Joint Constraints that Makes Natural Motion Possible: Experimental Verification on the Ankle", in Lenarčič, J. and Siciliano, B. (Eds.), *Advances in Robot Kinematics 2020*, Springer International Publishing, Cham, pp. 109–116, doi: 10.1007/978-3-030-50975-0_14.

Conconi, M., Sancisi, N. and Parenti-Castelli, V. (2021c), "Prediction of Individual Knee Kinematics From an MRI Representation of the Articular Surfaces", *IEEE Transactions on Biomedical Engineering*, Vol. 68 No. 3, pp. 1084–1092, doi: 10.1109/TBME.2020.3018113.

Conconi, M., Sancisi, N. and Parenti-Castelli, V. (2022a), "Exploiting Reciprocity Between Constraints and Instantaneous Motion to Reconstruct Individual Knee Kinematics", in Altuzarra, O. and Kecskeméthy, A. (Eds.), *Advances in Robot Kinematics 2022*, Springer International Publishing, Cham, pp. 367–374, doi: 10.1007/978-3-031-08140-8_40.

Conconi, M., Sancisi, N. and Parenti-Castelli, V. (2022b), "Exploiting Reciprocity Between Constraints and Instantaneous Motion to Reconstruct Individual Knee Kinematics", in Altuzarra, O. and Kecskeméthy, A. (Eds.), *Advances in Robot Kinematics 2022*, Springer International Publishing, Cham, pp. 367–374, doi: 10.1007/978-3-031-08140-8_40.

"Cupping blowout". (2020), *Formlabs.Com*, 15 September, available at: https://support.formlabs.com/s/article/Cupping-Blowout?language=en_US (accessed 19 February 2023).

Diment, L.E., Thompson, M.S. and Bergmann, J.H.M. (2017), "Clinical efficacy and effectiveness of 3D printing: a systematic review", *BMJ Open*, Vol. 7 No. 12, p. e016891, doi: 10.1136/bmjopen-2017-016891.

Erdemir, A., Besier, T.F., Halloran, J.P., Imhauser, C.W., Laz, P.J., Morrison, T.M. and Shelburne, K.B. (2019), "Deciphering the 'Art' in Modeling and Simulation of the Knee Joint: Overall Strategy", *Journal of Biomechanical Engineering*, Vol. 141 No. 7, doi: 10.1115/1.4043346.

Fleming, C., Sadaghiani, M.S., Stellon, M.A. and Javan, R. (2020), "Effectiveness of three-dimensionally printed models in anatomy education for medical students and resident physicians: systematic review and meta-analysis", *Journal of the American College of Radiology*, Elsevier, Vol. 17 No. 10, pp. 1220–1229.

Forlani, M., Sancisi, N., Conconi, M. and Parenti-Castelli, V. (2016), "A new test rig for static and dynamic evaluation of knee motion based on a cable-driven parallel manipulator loading system", *Meccanica*, Springer, Vol. 51, pp. 1571–1581.

Fuh, J.Y.H., Choo, Y.S., Lu, L., Nee, A.Y.C., Wong, Y.S., Wang, W.L., Miyazawa, T., *et al.* (1997), "Post-cure shrinkage of photo-sensitive material used in laser lithography process", *Journal of Materials Processing Technology*, Elsevier, Vol. 63 No. 1–3, pp. 887–891.

Gandhi, R., de Beer, J., Petruccelli, D. and Winemaker, M. (2007), "Does patient perception of alignment affect total knee arthroplasty outcome?", *Canadian Journal of Surgery*, Canadian Medical Association, Vol. 50 No. 3, p. 181.

Grood, E.S. and Suntay, W.J. (1983), "A Joint Coordinate System for the Clinical Description of Three-Dimensional Motions: Application to the Knee", *Journal of Biomechanical Engineering*, Vol. 105 No. 2, pp. 136–144, doi: 10.1115/1.3138397.

Gunaratne, R., Pratt, D.N., Banda, J., Fick, D.P., Khan, R.J.K. and Robertson, B.W. (2017a), "Patient Dissatisfaction Following Total Knee Arthroplasty: A Systematic Review of the Literature", *The Journal of Arthroplasty*, Vol. 32 No. 12, pp. 3854–3860, doi: 10.1016/j.arth.2017.07.021.

Gunaratne, R., Pratt, D.N., Banda, J., Fick, D.P., Khan, R.J.K. and Robertson, B.W. (2017b), "Patient Dissatisfaction Following Total Knee Arthroplasty: A Systematic Review of the Literature", *The Journal of Arthroplasty*, Vol. 32 No. 12, pp. 3854–3860, doi: https://doi.org/10.1016/j.arth.2017.07.021.

Jang, G., Kim, S.-K., Heo, S.-J. and Koak, J.-Y. (2023), "Fit analysis of stereolithography-manufactured three-unit resin prosthesis with different 3D-printing build orientations and layer thicknesses", *The Journal of Prosthetic Dentistry*, Elsevier.

Katheng, A., Kanazawa, M., Iwaki, M. and Minakuchi, S. (2021), "Evaluation of dimensional accuracy and degree of polymerization of stereolithography photopolymer resin under different postpolymerization conditions: an in vitro study", *The Journal of Prosthetic Dentistry*, Elsevier, Vol. 125 No. 4, pp. 695–702.

Kim, T.K., Chang, C.B., Kang, Y.G., Kim, S.J. and Seong, S.C. (2009), "Causes and Predictors of Patient's Dissatisfaction After Uncomplicated Total Knee Arthroplasty", *The Journal of Arthroplasty*, Vol. 24 No. 2, pp. 263–271, doi: 10.1016/j.arth.2007.11.005.

Lakkala, P., Munnangi, S.R., Bandari, S. and Repka, M. (2023), "Additive manufacturing technologies with emphasis on stereolithography 3D printing in pharmaceutical and medical applications: A review", *International Journal of Pharmaceutics: X*, Elsevier, p. 100159.

Langridge, B., Momin, S., Coumbe, B., Woin, E., Griffin, M. and Butler, P. (2018), "Systematic Review of the Use of 3-Dimensional Printing in Surgical Teaching and Assessment", *Journal of Surgical Education*, Vol. 75 No. 1, pp. 209–221, doi: 10.1016/j.jsurg.2017.06.033.

Martelli, S., Sancisi, N., Conconi, M., Pandy, M.G., Kersh, M.E., Parenti-Castelli, V. and Reynolds, K.J. (2020), "The relationship between tibiofemoral geometry and musculoskeletal function during normal activity", *Gait & Posture*, Vol. 80, pp. 374–382, doi: 10.1016/j.gaitpost.2020.06.022.

McCarty, M.C., Chen, S.J., English, J.D. and Kasper, F. (2020), "Effect of print orientation and duration of ultraviolet curing on the dimensional accuracy of a 3-dimensionally printed orthodontic clear aligner design", *American Journal of Orthodontics and Dentofacial Orthopedics*, Vol. 158 No. 6, pp. 889–897, doi: https://doi.org/10.1016/j.ajodo.2020.03.023.

Melchels, F.P.W., Feijen, J. and Grijpma, D.W. (2010), "A review on stereolithography and its applications in biomedical engineering", *Biomaterials*, Elsevier, Vol. 31 No. 24, pp. 6121–6130, doi: 10.1016/J.BIOMATERIALS.2010.04.050.

Mercader, A., Rottinger, T., Bigdeli, A., Rottinger, H. and Lueth, T.C. (2021), "A 3D Printed Mechanical Model of the Knee to Detect and Avoid Total Knee Replacement Surgery Errors", *2021 IEEE International Conference on Robotics and Automation (ICRA)*, IEEE, pp. 12501–12507, doi: 10.1109/ICRA48506.2021.9561403.

Nardini, F., Belvedere, C., Sancisi, N., Conconi, M., Leardini, A., Durante, S. and Parenti-Castelli, V. (2020a), "An Anatomical-Based Subject-Specific Model of In-Vivo Knee Joint 3D Kinematics From Medical Imaging", *Applied Sciences*, Vol. 10 No. 6, p. 2100, doi: 10.3390/app10062100.

Nardini, F., Belvedere, C., Sancisi, N., Conconi, M., Leardini, A., Durante, S. and Parenti-Castelli, V. (2020b), "An Anatomical-Based Subject-Specific Model of In-Vivo Knee Joint 3D Kinematics From Medical Imaging", *Applied Sciences*, Vol. 10 No. 6, p. 2100, doi: 10.3390/app10062100.

Ngo, T.D., Kashani, A., Imbalzano, G., Nguyen, K.T.Q. and Hui, D. (2018), "Additive manufacturing (3D printing): A review of materials, methods, applications and challenges", *Composites Part B: Engineering*, Elsevier, Vol. 143, pp. 172–196.

Noble, P.C., Conditt, M.A., Cook, K.F. and Mathis, K.B. (2006), "The John Insall Award: Patient expectations affect satisfaction with total knee arthroplasty.", *Clinical Orthopaedics and Related Research (1976-2007)*, LWW, Vol. 452, pp. 35–43.

Parenti-Castelli, V., Catani, F., Sancisi, N., & Leardini, A. (2010). Improved orthopaedic device. PCT Patent WO2010/128485.

Park, G.-S., Kim, S.-K., Heo, S.-J., Koak, J.-Y. and Seo, D.-G. (2019), "Effects of printing parameters on the fit of implant-supported 3D printing resin prosthetics", *Materials*, MDPI, Vol. 12 No. 16, p. 2533.

Raman, R. and Bashir, R. (2015), "Stereolithographic 3D bioprinting for biomedical applications", *Essentials of 3D Biofabrication and Translation*, Elsevier, pp. 89–121.

Schwartz, A.M., Farley, K.X., Guild, G.N. and Bradbury Jr, T.L. (2020), "Projections and epidemiology of revision hip and knee arthroplasty in the United States to 2030", *The Journal of Arthroplasty*, Elsevier, Vol. 35 No. 6, pp. S79–S85.

Scott, C.E.H., Howie, C.R., MacDonald, D. and Biant, L.C. (2010), "Predicting dissatisfaction following total knee replacement: a prospective study of 1217 patients", *The Journal of Bone & Joint Surgery British Volume*, Bone & Joint, Vol. 92 No. 9, pp. 1253–1258.

Sensini, A. and Cristofolini, L. (2018), "Biofabrication of electrospun scaffolds for the regeneration of tendons and ligaments", *Materials*, MDPI, Vol. 11 No. 10, p. 1963.

Sloan, M., Premkumar, A. and Sheth, N.P. (2018), "Projected Volume of Primary Total Joint Arthroplasty in the U.S., 2014 to 2030", *Journal of Bone and Joint Surgery*, Vol. 100 No. 17, pp. 1455–1460, doi: 10.2106/JBJS.17.01617.

Smith, C.F., Tollemache, N., Covill, D. and Johnston, M. (2018), "Take away body parts! An investigation into the use of 3D-printed anatomical models in undergraduate anatomy education", *Anatomical Sciences Education*, Vol. 11 No. 1, pp. 44–53, doi: 10.1002/ase.1718.

Tack, P., Victor, J., Gemmel, P. and Annemans, L. (2016), "3D-printing techniques in a medical setting: a systematic literature review", *BioMedical Engineering OnLine*, Vol. 15 No. 1, p. 115, doi: 10.1186/s12938-016-0236-4.

Tashman, S. and Anderst, W. (2003), "In-Vivo Measurement of Dynamic Joint Motion Using High Speed Biplane Radiography and CT: Application to Canine ACL Deficiency", *Journal of Biomechanical Engineering*, Vol. 125 No. 2, pp. 238–245, doi: 10.1115/1.1559896.

Unkovskiy, A., Bui, P.H.-B., Schille, C., Geis-Gerstorfer, J., Huettig, F. and Spintzyk, S. (2018), "Objects build orientation, positioning, and curing influence dimensional accuracy and flexural properties of stereolithographically printed resin", *Dental Materials*, Vol. 34 No. 12, pp. e324–e333, doi: 10.1016/j.dental.2018.09.011.

Wang, W.L., Cheah, C.M., Fuh, J.Y.H. and Lu, L. (1996), "Influence of process parameters on stereolithography part shrinkage", *Materials & Design*, Elsevier, Vol. 17 No. 4, pp. 205–213.

Windolf, M., Götzen, N. and Morlock, M. (2008), "Systematic accuracy and precision analysis of video motion capturing systems—exemplified on the Vicon-460 system", *Journal of Biomechanics*, Elsevier, Vol. 41 No. 12, pp. 2776–2780.

Wright, J.M., Ford, J.M., Qamar, F., Lee, M., Halsey, J.N., Smyth, M.D., Decker, S.J., *et al.* (2023), "Design and Validation of a 3D Printed Cranio-Facial Simulator: A Novel Tool for Surgical Education", *The Cleft Palate Craniofacial Journal*, SAGE Publications Sage CA: Los Angeles, CA, p. 10556656221151096.

Ye, Z., Dun, A., Jiang, H., Nie, C., Zhao, S., Wang, T. and Zhai, J. (2020), "The role of 3D printed models in the teaching of human anatomy: a systematic review and meta-analysis", *BMC Medical Education*, Vol. 20 No. 1, p. 335, doi: 10.1186/s12909-020-02242-x.

Zhao, J., Yang, Y. and Li, L. (2020), "A comprehensive evaluation for different post-curing methods used in stereolithography additive manufacturing", *Journal of Manufacturing Processes*, Elsevier, Vol. 56, pp. 867–877.